PHYSICAL REVIEW B **71**, 041406(R) (2005)

Disorder and interaction effects in two-dimensional graphene sheets

T. Stauber, F. Guinea, and M. A. H. Vozmediano*
Instituto de Ciencia de Materiales de Madrid, CSIC, Cantoblanco, E-28049 Madrid, Spain
(Received 24 September 2004; published 25 January 2005)

The interplay between different types of disorder and electron-electron interactions in graphene planes is studied by means of renormalization group techniques. The low-temperature properties of the system are determined by fixed points where the strength of the interactions remains finite, as in one-dimensional Luttinger liquids. These fixed points can be either stable, when the disorder is associated to topological defects in the lattice or to a random mass term, or unstable when the disorder is induced by impurities outside the graphene planes.

DOI: 10.1103/PhysRevB.71.041406 PACS number(s): 81.05.Uw, 75.10.Jm, 75.10.Lp, 75.30.Ds

I. INTRODUCTION

Graphite is a widely studied material, which has attracted recent interest due to the observation of many anomalous transport properties[1–8] and, most exciting, the report of magnetism at room temperatures.[9]

The conduction band of graphite is well described by tight-binding models which include only the π orbitals which are perpendicular to the graphite planes at each C atom.[10] If the interplane hopping is neglected, this model describes a semimetal, with zero density of states at the Fermi energy, and where the Fermi surface is reduced to two inequivalent points in the Brillouin zone. The states near these Fermi points can be described by a continuum model which reduces to the Dirac equation in two dimensions. Due to the vanishing of the density of states at the Fermi level, the long-range Coulomb interaction is imperfectly screened. This implies that a standard perturbative treatment leads to logarithmic divergences, and to nontrivial deviations from Fermi-liquid theory.[11–13] Short-range interactions responsible for ferromagnetic effects are irrelevant in this context due to the vanishing density of states at the Fermi level. In the strong coupling regime, the model can exhibit a phase transition which leads to a rearrangement of the charges and spins within the unit cell, and which is similar to the chiral symmetry breaking transition found in field theories.[14,15] The experimental findings are hard to explain within this exponentially weak nonperturbative effect.

It is known that disorder significantly changes the states described by the two-dimensional Dirac equation,[16–18] and, usually, the density of states at low energies is increased. Lattice defects, such as pentagons and heptagons, or dislocations, can be included in the continuunm model by means of a non-Abelian gauge field.[19,20] In general, disorder enhances the short-range interactions. In addition, a graphene plane can show states localized at interfaces,[21,22] which, in the absence of other types of disorder, lie at the Fermi energy. Changes in the local coordination can also lead to localized states.[23]

The present work studies the inteplay of long-range interactions and disorder in the two-dimensional graphene plane aiming to open a way for describing the experimental findings. This problem has already been studied in the context of critical points between integer and fractional fillings in the quantum Hall effect,[24–26] and we will be able to translate some of the results there to the problem at hand. We find, as in Ref. 26 a rich phase diagram, with different fixed points. The stability of these fixed points depends on the nature of the disorder.

II. THE MODEL: COULOMB INTERACTION AND DISORDER

We describe the electronic states within each graphene plane by two two-component spinors associated to the two inequivalent Fermi points in the Brillouin zone. They are combined to a four-component (Dirac) spinor. These spinors obey the massless Dirac equation. The Hamiltonian of the free system is

$$H_0 = iv_F \int d^2x \overline{\Psi}(\vec{x}) \vec{\gamma} \cdot \vec{\nabla} \Psi(\vec{x}), \tag{1}$$

where $\overline{\Psi} \equiv \Psi^\dagger \gamma_0$ with the 4×4 matrix $\gamma_0 \equiv \sigma_3 \otimes \sigma_3$. We further have $\vec{\gamma} \equiv (\gamma_1, \gamma_2) = (-i\sigma_2, i\sigma_1) \otimes \sigma_3$. The σ_μ denote the usual Pauli matrices such that $\{\gamma_\mu, \gamma_\nu\} = 2g_{\mu,\nu} 1_{4\times 4}$, $g_{\mu,\nu}$ denoting the Minkowski tensor, where $g_{0,0}=1$, $g_{i,i}=-1$ with $i=1,2$, and zero otherwise.

The long-range Coulomb interaction in terms of the Dirac spinors reads

$$H_{ee} = \frac{v_F}{4\pi} \int d^2x d^2x' \overline{\Psi}(\vec{x}) \gamma_0 \Psi(\vec{x}) \frac{g}{|\vec{x}-\vec{x}'|} \overline{\Psi}(\vec{x}') \gamma_0 \Psi(\vec{x}'), \tag{2}$$

where $g = e^2/v_F$ is the dimensionless coupling constant.

In order to describe disorder effects, the Dirac spinors are coupled to a gauge field $A(\vec{x})$,

$$H_{disorder} = \frac{v_\Gamma}{4} \int d^2x \overline{\Psi}(\vec{x}) \Gamma \Psi(\vec{x}) A(\vec{x}), \tag{3}$$

where v_Γ characterizes the strength and the 4×4 matrix Γ the type of the vertex. In general, $A(\vec{x})$ is a quenched, Gaussian variable with the dimensionless variance Δ, i.e.,

$$\langle A(\vec{x}) \rangle = 0 \quad \langle A(\vec{x}) A(\vec{x}') \rangle = \Delta \delta^2(\vec{x}-\vec{x}'). \tag{4}$$

We will discuss five different types of disorder which are associated to the five mutually anticommuting 4×4 matrices

plus the unity matrix: (i) For a random chemical potential, the 4×4 matrix Γ is given by $\Gamma=\gamma_0$. The long-range components of this type of disorder do not induce transitions between the two inequivalent Fermi points. This type of disorder will yield an unstable fixed line. (ii) A random gauge potential involves the 4×4 matrices $\Gamma=i\gamma_1$ and $\Gamma=i\gamma_2$. This type of disorder will yield a stable fixed line which is linear in the (g,Δ)-plane. (iii) (a) A fluctuating mass term is described by $\Gamma=1_{4\times4}$. (b) Topological disorder is given by $\Gamma=i\gamma_5$ with $\gamma_5=1_{2\times2}\otimes\sigma_2$. This type of disorder is associated to the existence of pentagons and heptagons, or, more generally, to local distortions of the lattice axes.[19,20] This term can thus be represented by a gauge potential which induces transitions between the two Fermi points. (c) To complete the discussion, we also mention $\Gamma=i\tilde{\gamma}_5$, where $\tilde{\gamma}_5=1_{2\times2}\otimes\sigma_1$. This vertex type can be related to an imaginary mass that couples the two inequivalent Fermi points. All these types of disorder will yield a stable fixed line which is cubic in the (g,Δ)-plane.

III. RENORMALIZATION OF THE EFFECTIVE COUPLINGS

To discuss the renormalizability of the theory, we will first treat the disorder gauge field as an external potential and do not consider the average over different realizations of this field. The free, massless Dirac propagator is given by[12]

$$G_0(\omega,\vec{p}) = -i\int\frac{d\omega}{2\pi}\frac{d^2p}{(2\pi)^2}e^{i\omega t-i\vec{p}\vec{x}}\langle T\Psi(t,\vec{x})\overline{\Psi}(0,0)\rangle$$
$$=\frac{-1}{\gamma_0\omega-v_F\vec{\gamma}\cdot\vec{p}+i0}. \tag{5}$$

Within one loop and without averaging over the disorder potential, only two diagrams need to be considered, i.e., the self-energy of the fermion propagator due to electron-electron interaction and the vertex correction of the "external" gauge field that couples to the Dirac bilinear $\overline{\Psi}\Gamma\Psi$. Both diagrams are shown on the left-hand side of Fig. 1.

The Fermi velocity is renormalized by the top left diagram of Fig. 1 as $v_F=Z_{v_F}\tilde{v}_F$ with $Z_{v_F}=1-g/(16\pi\varepsilon)$, using dimensional regularization with $\varepsilon\to0$.[12] Notice that the vertex of the Coulomb interaction is not renormalized within one-loop order.

Whether or not v_Γ needs to be renormalized depends on the type of the disorder: (i) For a random chemical potential with $\Gamma=\gamma_0$, the right diagram at the top of Fig. 1 is nondivergent. This statement is equivalent to the one that there is no vertex correction of the Coulomb interaction. We thus set $v_\Gamma=v_1$ with the flow-invariant velocity v_1. (ii) For a random gauge potential $(\Gamma=i\gamma_1,i\gamma_2)$, the vertex is renormalized by the same factor as the Fermi velocity, i.e., $Z_\Gamma=1-g/(16\pi\varepsilon)$. This fact is related to the conservation of the current. We can thus set $v_\Gamma=v_F$. (iii) For a random mass term $\Gamma=1_{4\times4}$, topological disorder $\Gamma=i\gamma_5$, and $\Gamma=i\tilde{\gamma}_5$, the vertex strength v_Γ is renormalized by $Z_\Gamma=1-g/(8\pi\varepsilon)$ which follows from (i) and (ii). Within one loop-level, we can thus set $v_\Gamma=v_F^2/v_3$ with the flow-invariant velocity v_3.

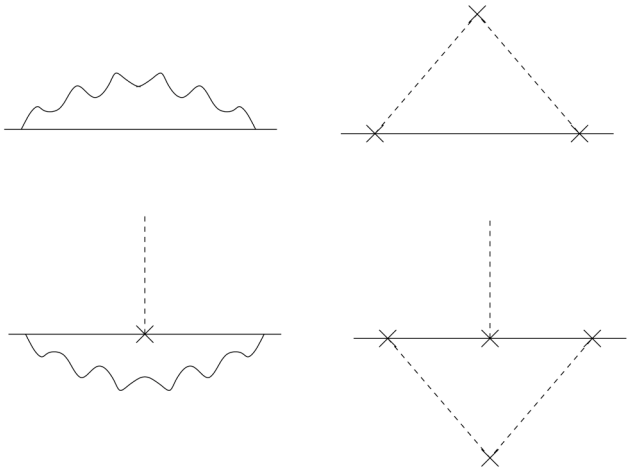

FIG. 1. Top, self-energy corrections. Dashed line, Coulomb interaction. Dotted line, external disorder. Bottom: renormalization of the vertex for the external disorder.

IV. AVERAGING OVER DISORDER

As it was discussed in Ref. 12, there is no wave function renormalization Z_Ψ to leading order in g. Including self-energy corrections due to averaging over an ensemble of various realizations of the gauge field $A(\vec{x})$, the wave function gets renormalized.[20] The self-energy due to disorder is shown at the top right of Fig. 1 and reads

$$\Sigma_\Gamma(\omega)=\Delta\frac{v_\Gamma^2}{16}\int\frac{d^2p}{(2\pi)^2}\Gamma G_0(\omega,\vec{p})\Gamma. \tag{6}$$

The wave function renormalization is independent of the vertex type and yields $Z_\Psi=1-\Delta v_\Gamma^2/(32\pi v_F^2\varepsilon)$, where again we use dimensional regularization with $\varepsilon\to0$.

The wave function renormalization Z_Ψ also changes the renormalization factor of the Fermi velocity as we keep $G_{0,Z}^{-1}-\Sigma$ invariant with

$$G_{0,Z}^{-1}(\omega,\vec{p})\equiv-Z_\Psi(\gamma_0\omega-Z_{v_F}v_F\vec{\gamma}\cdot\vec{p}). \tag{7}$$

We also need to discuss the vertex corrections due to averaging over the disorder. The diagram which renormalizes the vertex of the external gauge field is shown at the bottom of Fig. 1. Also the vertex of the Coulomb interaction is being renormalized (not shown). The vertex correction to Γ due to averaging over the disorder type Γ' is given by

$$V_\Gamma(\omega,\vec{k})=\Delta\frac{v_{\Gamma'}^2}{16}\int\frac{d^2p}{(2\pi)^2}\Gamma' G_0(\omega,\vec{p})\Gamma G_0(\omega,\vec{p}+\vec{k})\Gamma'. \tag{8}$$

This expression depends on the given combination of vertices. The electric charge is not renormalized. If there is only one type of disorder, the vertex correction exactly compensates the effect of Z_ψ on Z_{v_F} so that the identification of the vertex of the external potential and the Fermi velocity remains valid, i.e., (i) $v_\Gamma=v_1$, (ii) $v_\Gamma=v_F$, and (iii) $v_\Gamma=v_F^2/v_3$ with v_1, v_3 constant.

V. PHASE DIAGRAMS

Disorder thus only changes the flow of the Fermi velocity due to wave function renormalization, i.e., $Z_{v_F} \to Z_{v_F}/Z_\Psi$. From the β-function $\beta_{v_F} = \Lambda \partial_\Lambda Z_{v_F} \tilde{v}_F$, we obtain the following flow equation for the effective Fermi velocity v_F^{eff} ($\ell = \ln \Lambda/\Lambda_0 \sim 1/\varepsilon$):

$$\frac{d}{d\ell}\frac{v_F^{eff}}{\tilde{v}_F} = \frac{1}{16\pi}\left[\frac{e^2}{v_F^{eff}} - \frac{\Delta}{2}\left(\frac{v_\Gamma^{eff}}{v_F^{eff}}\right)^2\right]. \tag{9}$$

We can now discuss the phase diagram for the various types of disorder: (i) For a random chemical potential ($\Gamma = \gamma_0$), $v_\Gamma = v_1$ remains constant under renormalization group transformation. There is thus an unstable fixed line at $v_F^* = v_1^2 \Delta/(2e^2)$. In the (g, Δ)-plane, the strong-coupling and the weak-coupling phases are separated by a hyperbola, with the critical electron interaction $g^* = e^2/v_F^* = 2e^4/(v_1^2\Delta)$. (ii) A random gauge potential involves the vertices $\Gamma = i\gamma_1, i\gamma_2$. The vertex strength renormalizes as $v_\Gamma = v_F$. There is thus an attractive Luttinger-like fixed point for each disorder correlation strength Δ given by $v_F^* = 2e^2/\Delta$ or $g^* = \Delta/2$. (iii) For a random mass term $\Gamma = 1_{4\times4}$, topological disorder $\Gamma = i\gamma_5$, and $\Gamma = i\tilde{\gamma}_5$, we have $v_\Gamma = v_F^2/v_3$. There is thus again an attractive Luttinger-like fixed point for each disorder correlation strength Δ given by $v_F^* = \sqrt[3]{2v_3^2 e^2/\Delta}$ or $g^* = \sqrt[3]{\Delta e^4/(2v_3^2)}$.

To make connection to previous work,[26] we define $\tilde{\Delta} \equiv (\Delta/2)(v_\Gamma^{eff}/v_F^{eff})^2$. This yields the linear fixed line $g^* = \tilde{\Delta}$ with (i) $\tilde{\Delta} \propto g^2$, (ii) $\tilde{\Delta} \propto$ const, and (iii) $\tilde{\Delta} \propto g^{-2}$. For each disorder type, our results agree with those in Ref. 26.

VI. VARIOUS DISORDER TYPES

Various disorder types cause the renormalization flow to become unstable which was first noticed by Ludwig *et al.* for the system without electron-electron interaction.[24] Still, we expect that the generic flow of the phase diagram with one disorder type remains valid as long as one is far enough away from the fixed line. To support this assumption, we will discuss the system with two disorder types present.

Let us, e.g., consider the potential disorder Δ_V and the gauge potential disorder Δ_A. Then, the disorder strength v_Γ with $\Gamma = \gamma_0$ still does not flow under the renormalization group (RG) transformation, but the identification of the disorder strength v_Γ with $\Gamma = i\gamma_1, i\gamma_2$ with the Fermi velocity is not valid anymore.

Let us parametrize the velocity of the disorder $\Gamma = i\gamma_1, i\gamma_2$ as $v_\Gamma = v_F + \delta v$, where δv is the deviation of the Fermi velocity due to the presence of the potential disorder Δ_V. The flow equation of the effective deviation δv^{eff} then reads

$$\frac{d}{d\ell}\frac{\delta v^{eff}}{\tilde{v}_F} = \frac{1}{32\pi}\frac{\Delta_V}{(v_F^{eff})^2}. \tag{10}$$

There is thus a monotonic increase of the deviation δv^{eff} which in return causes the Fermi velocity to decrease. All together, we expect that the phase diagram in the middle of Fig. 2 remains valid for points for away from the attractive fixed line. Close the the attractor, the former fixed line becomes unstable and there is a flow towards the strong coupling regime in the direction of the former fixed line.

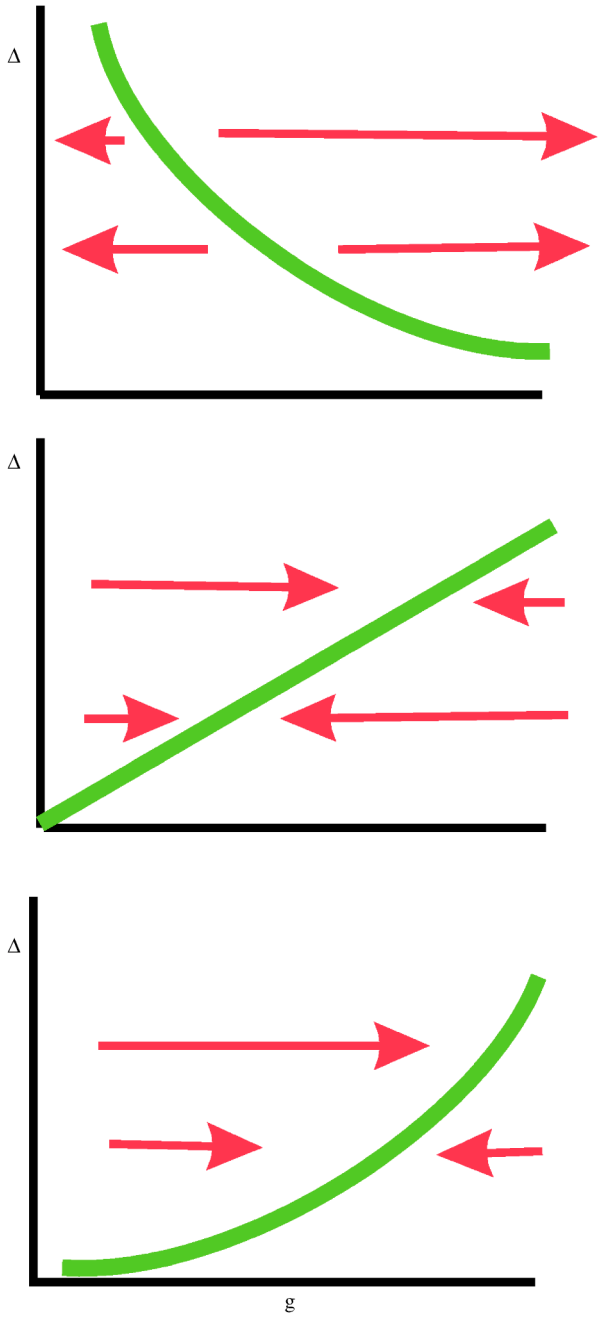

FIG. 2. (Color online) One-loop phase diagram for two-dimensional massless Dirac spinors including long-ranged electron-electron interaction g and disorder Δ. Top, random chemical potential ($\Gamma = \gamma_0$). Center, random gauge potential ($\Gamma = i\gamma_1, i\gamma_2$). Bottom, random mass term ($\Gamma = 1_{4\times4}$), topological disorder ($\Gamma = i\gamma_5$), and $\Gamma = i\tilde{\gamma}_5$.

For a general combination of disorder types, we expect a similar behavior, i.e., close to the phase separation there will be a flow towards the strong coupling regime where our one-loop renormalization analysis breaks down.

VII. CONCLUSIONS

In this work, we explored the phase diagram of a microscopic model for two-dimensional graphene sheets in the presence of long-ranged electron-electron interaction and disorder. Disorder is modeled as in the quantum Hall transitions, by five different vertices which lead—within a one-loop level—to a very rich phase diagram. A random gauge potential as well as a random mass term and topological disorder drive the system towards a new stable, Luttinger-like fixed point. This phase is characterized by a vanishing quasiparticle residue, leading to anomalous one-particle properties. The Luttinger liquid features associated to this fixed line are notoriously difficult to observe, although they can be probed in tunneling experiments, or by measuring the peak width in ARPES. They will also influence the interlayer transport properties.[27,28] Small perturbations by other types of disorder, such as a random local potential induce a flow along this fixed line, as in the absence of interactions.[24] The strong coupling fixed point describes, most likely, a disordered insulating system.

Being a weak coupling RG calculation, the phase diagrams discussed here can only give a qualitative picture of the variety of phases which can be induced by the interplay of interactions and disorder. In the absence of disorder the electronic charge flows towards weak coupling even when a high-order resummation of diagrams is performed, valid in the strong coupling case,[13] so that our results should be generally valid when the disorder is weak. We can estimate the strength of the types of defect considered here by noting that randomness in the chemical potential, due to local defects, such as impurities or vacancies, lead to $\Delta \sim (V/\hbar v_F)^2 c$, where V is the strength of the local potential and c is the concentration, so that $\Delta \sim ca^2$ for vacancies, where a is the lattice constant. Lattice defects, such as dislocations, induce an effective gauge potential with $\Delta \sim cb^2$,[20] where b is the Burgers vector of the dislocation and c is the concentration. These defects can be induced by irradiation.[9] Note that the presence of disorder at intermediate scales will suppress the chiral symmetry breaking transition expected for pure graphene[14,15] leaving disorder as the most probable effect for describing the phenomena.

ACKNOWLEDGMENTS

T.S. was financially supported by DAAD. Funding from MCyT (Spain) through Grant No. MAT2002-0495-C02-01 was also acknowledged. M.A.H.V. thanks A. Ludwig and C. Mudry for very useful conversations on disordered systems, and the Aspen Institute of Physics where these issues were discussed for its hospitality. We also thank P. Esquinazi for many illuminating discussions.

*Present address: Departamento de Matemáticas, Universidad Carlos, III de Madrid, E-28911 Leganés, Madrid, Spain

[1] Y. Kopelevich, P. Esquinazi, J. H. S. Torres, and S. Moehlecke, J. Low Temp. Phys. **119**, 691 (2000).
[2] P. Esquinazi, A. Setzer, R. Höhne, C. Semmelhack, Y. Kopelevich, D. Spemann, T. Butz, B. Kohlstrunk, and M. Lösche, Phys. Rev. B **66**, 024429 (2002).
[3] H. Kempa, P. Esquinazi, and Y. Kopelevich, Phys. Rev. B **65**, 241101 (2002).
[4] Y. Kopelevich, P. Esquinazi, J. H. S. Torres, R. R. da Silva, and H. Kempa, in *Studies of High Temperature Superconductors*, edited by A. Narlikar (Nova Science, Hauppauge, NY, 2003), Vol. 45, p. 59.
[5] S. Moehlecke, P.-C. Ho, and M. B. Maple, Philos. Mag. Lett. **82**, 1335 (2002).
[6] J. M. D. Coey, M. Venkatesan, C. B. Fitzgerald, A. P. Douvalis, and I. S. Sanders, Nature (London) **420**, 156 (2002).
[7] Y. Kopelevich, J. H. S. Torres, R. R. da Silva, F. Mrowka, H. Kempa, and P. Esquinazi, Phys. Rev. Lett. **90**, 156402 (2003).
[8] H. Kempa, H. C. Semmelhack, P. Esquinazi, and Y. Kopelevich, Solid State Commun. **125**, 1 (2003).
[9] P. Esquinazi, D. Spemann, R. Höhne, A. Setzer, K.-H. Han, and T. Butz, Phys. Rev. Lett. **91**, 227201 (2003).
[10] J. C. Slonczewski and P. R. Weiss, Phys. Rev. **109**, 272 (1958).
[11] J. González, F. Guinea, and M. A. H. Vozmediano, Mod. Phys. Lett. B **7**, 1593 (1993).
[12] J. González, F. Guinea, and M. A. H. Vozmediano, Nucl. Phys. B **424 [FS]**, 595 (1994).
[13] J. González, F. Guinea, and M. A. H. Vozmediano, Phys. Rev. B **59**, R2474 (1999).
[14] D. V. Khveshchenko, Phys. Rev. Lett. **87**, 246802 (2001).
[15] D. V. Khveshchenko, Phys. Rev. Lett. **87**, 206401 (2001).
[16] C. de C. Chamon, C. Mudry, and X.-G. Wen, Phys. Rev. B **53**, R7638 (1996).
[17] H. E. Castillo, C. de C. Chamon, E. Fradkin, P. M. Goldbart, and C. Mudry, Phys. Rev. B **56**, 10668 (1997).
[18] B. Horovitz and P. Le Doussal, Phys. Rev. B **65**, 125323 (2002).
[19] J. González, F. Guinea, and M. A. H. Vozmediano, Nucl. Phys. B **406 [FS]**, 771 (1993).
[20] J. González, F. Guinea, and M. A. H. Vozmediano, Phys. Rev. B **63**, 134421 (2001).
[21] K. Wakabayashi and M. Sigrist, Phys. Rev. Lett. **84**, 3390 (2000).
[22] K. Wakabayashi, Phys. Rev. B **64**, 125428 (2001).
[23] A. A. Ovchinnikov and I. L. Shamovsky, J. Mol. Struct.: THEOCHEM **251**, 133 (1991).
[24] A. W. W. Ludwig, M. P. A. Fisher, R. Shankar, and G. Grinstein, Phys. Rev. B **50**, 7526 (1994).
[25] J. Ye and S. Sachdev, Phys. Rev. Lett. **80**, 5409 (1998).
[26] J. Ye, Phys. Rev. B **60**, 8290 (1999).
[27] M. A. H. Vozmediano, M. P. López-Sancho, and F. Guinea, Phys. Rev. Lett. **89**, 166401 (2002).
[28] M. A. H. Vozmediano, M. P. López-Sancho, and F. Guinea, Phys. Rev. B **68**, 195122 (2003).